The Plant Cell, Vol. 18, 3145–3157, November 2006, www.plantcell.org © 2006 American Society of Plant Biologists

SIAMESE, a Plant-Specific Cell Cycle Regulator, Controls Endoreplication Onset in *Arabidopsis thaliana* [W]

Michelle L. Churchman,[a,1] Matthew L. Brown,[a,1,2] Naohiro Kato,[a] Viktor Kirik,[b] Martin Hülskamp,[b] Dirk Inzé,[c] Lieven De Veylder,[c] Jason D. Walker,[a,3] Zhengui Zheng,[d] David G. Oppenheimer,[d] Taylor Gwin,[a] Jason Churchman,[a] and John C. Larkin[a,4]

[a] Department of Biological Sciences, Louisiana State University, Baton Rouge, Louisiana 70803
[b] University of Köln, Botanical Institute III, 50931 Köln, Germany
[c] Department of Plant Systems Biology, Flanders Interuniversitaru Instititut for Biotechnology, Ghent University, B-9000 Ghent, Belgium
[d] Department of Botany, Genetics Institute and Plant Molecular and Cell Biology Program, University of Florida, Gainesville, Florida 32611

Recessive mutations in the *SIAMESE* (*SIM*) gene of *Arabidopsis thaliana* result in multicellular trichomes harboring individual nuclei with a low ploidy level, a phenotype strikingly different from that of wild-type trichomes, which are single cells with a nuclear DNA content of ~16C to 32C. These observations suggested that *SIM* is required to suppress mitosis as part of the switch to endoreplication in trichomes. Here, we demonstrate that *SIM* encodes a nuclear-localized 14-kD protein containing a cyclin binding motif and a motif found in ICK/KRP (for Interactors of Cdc2 kinase/Kip-related protein) cell cycle inhibitor proteins. Accordingly, SIM was found to associate with D-type cyclins and CDKA;1. Homologs of SIM were detected in other dicots and in monocots but not in mammals or fungi. SIM proteins are expressed throughout the shoot apical meristem, in leaf primordia, and in the elongation zone of the root and are localized to the nucleus. Plants overexpressing SIM are slow-growing and have narrow leaves and enlarged epidermal cells with an increased DNA content resulting from additional endocycles. We hypothesize that SIM encodes a plant-specific CDK inhibitor with a key function in the mitosis-to-endoreplication transition.

INTRODUCTION

Cell differentiation is closely coordinated with cell cycle progression. In the simplest case, the cell cycle arrests concomitant with the onset of differentiation, but in many cell differentiation pathways, alternative versions of the cell cycle occur along with differentiation. One example is the altered division potential of transient amplifying cells, which are restricted in both their developmental potential and the number of times they can divide, relative to the undifferentiated and essentially immortal stem cells from which they derive (Watt and Hogan, 2000). Another example, common in both plants and animals, is the amplification of nuclear DNA by endocycles that continues during differentiation of many cell types, a process called either endoreplication or endoreduplication (Edgar and Orr-Weaver, 2001; Larkins et al., 2001). The coordination of these modified cell cycles with differentiation remains poorly understood.

[1] These authors contributed equally to this work.
[2] Current address: Department of Biotechnology and Molecular Medicine, School of Veterinary Medicine, Louisiana State University, Baton Rouge, LA 70803.
[3] Current address: Department of Biological and Biomedical Sciences, Yale University, New Haven, CT 06520.
[4] To whom correspondence should be addressed. E-mail jlarkin@lsu.edu; fax 225-578-2597.
The author responsible for distribution of materials integral to the findings presented in this article in accordance with the policy described in the Instructions for Authors (www.plantcell.org) is: John C. Larkin (jlarkin@lsu.edu).
[W] Online version contains Web-only data.
www.plantcell.org/cgi/doi/10.1105/tpc.106.044834

The regulation of cell cycle transitions in plants is similar to that of animals (reviewed in De Veylder et al., 2003; Dewitte and Murray, 2003; Inzé, 2005). Transitions between stages in the cell cycle are controlled by a class of Ser/Thr kinases known as cyclin-dependant kinases (CDKs). As suggested by their name, the kinase activity of CDKs depends on their association with a regulatory cyclin (CYC) protein. Cell cycle progression is regulated by periodic expression of cyclins and their ubiquitin-mediated proteolysis and by the phosphorylation of a variety of targets by CDK/cyclin complexes. The G1/S transition is regulated by phosphorylation of the retinoblastoma-related protein by a CDKA/CYCD complex. The G2/M transition most likely requires both A-type and B-type CDKs, as well as CYCA and CYCB proteins, to form mitotic CYC/CDK complexes (De Veylder et al., 2003; Dewitte and Murray, 2003; Inzé, 2005).

Cell cycle progression is also regulated by inhibitors of CYC/CDK complexes. The only plant CDK inhibitors identified to date are a family of proteins distantly related to the Kip family of animal CDK inhibitors; these proteins are known as Kip-related proteins (KRPs) (De Veylder et al., 2001) or Interactors of Cdc2 kinases (ICKs) (Wang et al., 1997). ICK/KRP proteins are generally thought to interact with CDKA and CYCDs (Wang et al., 1998; De Veylder et al., 2001), although two recent reports indicate that some family members may interact with CDKB as well (Nakai et al., 2006; Pettko-Szandtner et al., 2006). ICK/KRP proteins can inhibit CDK-associated histone H1 kinase activity in vitro or in vivo (Wang et al., 1997, 1998; De Veylder et al., 2001). Overproduction of these proteins in transgenic plants suppresses cell proliferation while increasing the length of the cell cycle and cell

size, resulting in smaller plants with serrated leaves (Wang et al., 2000; De Veylder et al., 2001). ICK/KRP overexpression differentially affects DNA content depending on the level of overexpression. Weak overexpression increases DNA content, while strong overexpression decreases DNA content (Verkest et al., 2005; Weinl et al., 2005). Together, these results suggest concentration-dependent roles for ICK/KRPs in blocking the G1/S cell cycle and blocking entry into mitosis but allowing S-phase progression.

During endoreplication cycles (endocycles), nuclear DNA is replicated without cytokinesis, resulting in cells with a DNA content greater than 2C. In angiosperms, endoreplication is particularly common and occurs in a wide variety of tissues and cell types, including agriculturally important tissues, such as maize (*Zea mays*) endosperm and cotton (*Gossypium hirsutum*) fibers (Kowles and Phillips, 1985; Van't Hof, 1999). Often, there is a correlation between the final volume of a differentiated cell and its DNA content (Melaragno et al., 1993; Hülskamp et al., 1994; Vlieghe et al., 2005). It is generally assumed that the function of endoreplication is gene amplification to supply the gene expression needs of large cells, but other explanations have been suggested (Nagl, 1976; Barlow, 1978). The primary functional features of the endocycle appear to be the absence of G2/M phase CDK activity, preventing mitosis, coupled with oscillations of G1/S CDK activity to allow relicensing of replication origins between each round of DNA replication (reviewed in Larkins et al., 2001). In maize endosperm, biochemical evidence has been obtained for two separable endoreplication-promoting factors: an activity inhibiting mitosis and an increase in S-phase-related protein kinase activity (Grafi and Larkins, 1995). Switching to endoreplication appears to involve downregulation of expression of CYCAs, CYCBs, and CDKB and activation of the anaphase promoting complex, which targets mitotic cyclins for degradation (reviewed in Dewitte and Murray, 2003; Inzé, 2005).

The shoot epidermal hairs (trichomes) of *Arabidopsis thaliana* are now well established as a model for the study of the plant cell cycle and cell differentiation. These trichomes are specialized branched single cells that extend out from the epidermis. During differentiation, trichome nuclei undergo endoreplication, resulting in a nuclear DNA content of 16C to 32C (Melaragno et al., 1993; Hülskamp et al., 1994). Mutations exist that either increase or decrease the nuclear DNA content (Perazza et al., 1999), including *KAKTUS*, *GLABRA3* (*GL3*), and *TRIPTYCHON*, which encode a HECT-class ubiquitin E3 ligase (El Refy et al., 2003), a basic helix-loop-helix transcription factor (Payne et al., 2000), and an inhibitory Myb transcription factor, respectively (Hülskamp et al., 1994). Recessive mutations in the *SIAMESE* (*SIM*) gene of *Arabidopsis* have a unique cell cycle–related phenotype, the production of multicellular trichomes, the individual nuclei of which have reduced levels of endoreplication (Walker et al., 2000). These observations suggest that *SIM* is required to suppress mitosis as part of the switch to endoreplication in trichomes.

In this study, we report that *SIM* encodes a 14-kD protein that is part of a small *Arabidopsis* gene family comprised of four members. Homologs exist in other dicots and in monocots, though no obvious animal homologs have been identified. These proteins share one motif with the ICK/KRP cell cycle inhibitor proteins and have a potential cyclin binding motif. We identified protein–protein interactions between SIM and D-type cylins as well as CDKA;1. *SIM* overexpression in transgenic plants results in small plants with serrated leaves containing enlarged cells with increased levels of nuclear DNA. Taken together, the *SIM* loss-of-function and gain-of-function phenotypes clearly point to an integral role for SIM in regulation of endoreplication.

RESULTS

Isolation of *SIM*

Wild-type trichomes are unicellular and occur singly on the leaf (Figure 1A). Three independent recessive *sim* mutant alleles have an essentially identical mutant phenotype of frequent multicellular trichomes and clusters of adjacent trichomes (Figures 1B and 1C). The *sim-1* mutation was mapped to a region of ~407 kb on chromosome five. Two markers located 66.5 kb apart on the overlapping BAC clones T32M21 and T19N18 showed no recombination in 1088 F2 chromosomes. Further attempts to reduce the genetic interval were unsuccessful. The *sim-2* allele originated in a T-DNA insertion population (Campisi et al., 1999). One of the two inserts present in the original *sim-2* T-DNA line showed linkage between the *sim* mutant phenotype and to both kanamycin resistance and β-glucuronidase (GUS) expression from an enhancer trap contained in the T-DNA. The right border of this T-DNA was obtained by adaptor PCR and shown by DNA sequencing to be positioned 1189 bp upstream of the coding region of the gene At5g04470, a gene located on the T32M21 BAC clone. The left border was located 1461 bp downstream, within the At5g04470 coding region, resulting in a deletion of these upstream sequences and the first 272 bp of the At5g04470 coding region (Figure 2A). Sequencing of this gene for the original *sim-1* allele revealed a point mutation changing the putative At5g04470 start codon from ATG to ATA, and a third allele, *sim-3*, contained a C→T mutation, resulting in a Pro-to-Ser amino acid change at position 36 (Figure 2A). In RT-PCR experiments, At5g04470 transcripts were detected in wild-type developing leaves but not in RNA isolated from the *sim-2* deletion allele (see Supplemental Figure 1 online). Finally, the *sim-1* mutant phenotype was rescued by the At5g04470 coding region under control of the trichome-specific *GL2* promoter (Figure 1D) and by a genomic DNA fragment including 2870 bp upstream of the At5g04470 start codon, the entire coding region, and 250 bp downstream of the stop codon (Figure 1E). Taken together, these results established that At5g04470 is the *SIM* gene and that *sim-1* and *sim-2* are likely to be amorphic alleles.

Conceptual translation of the open reading frame reveals that *SIM* encodes a 14-kD protein of unknown function. The SIM gene family of *Arabidopsis* contains at least four members, and homologs exist in other plant species, including both monocots and dicots (Figure 2B). Although SIM has no overall similarity with proteins of known function, several conserved motifs give clues as to its function. Motif 4 of the SIM family is similar to motif 3 of the CDK-inhibitory ICK/KRP proteins (De Veylder et al., 2001; Figures 2B and 2C). Motif 3 of the SIM family (Figure 2B) is a putative cyclin binding motif known as the Cy or zRxL motif, where Z is basic or Cys, and X is usually a basic residue. This motif is implicated in binding of some CDK inhibitors, E2F and RB

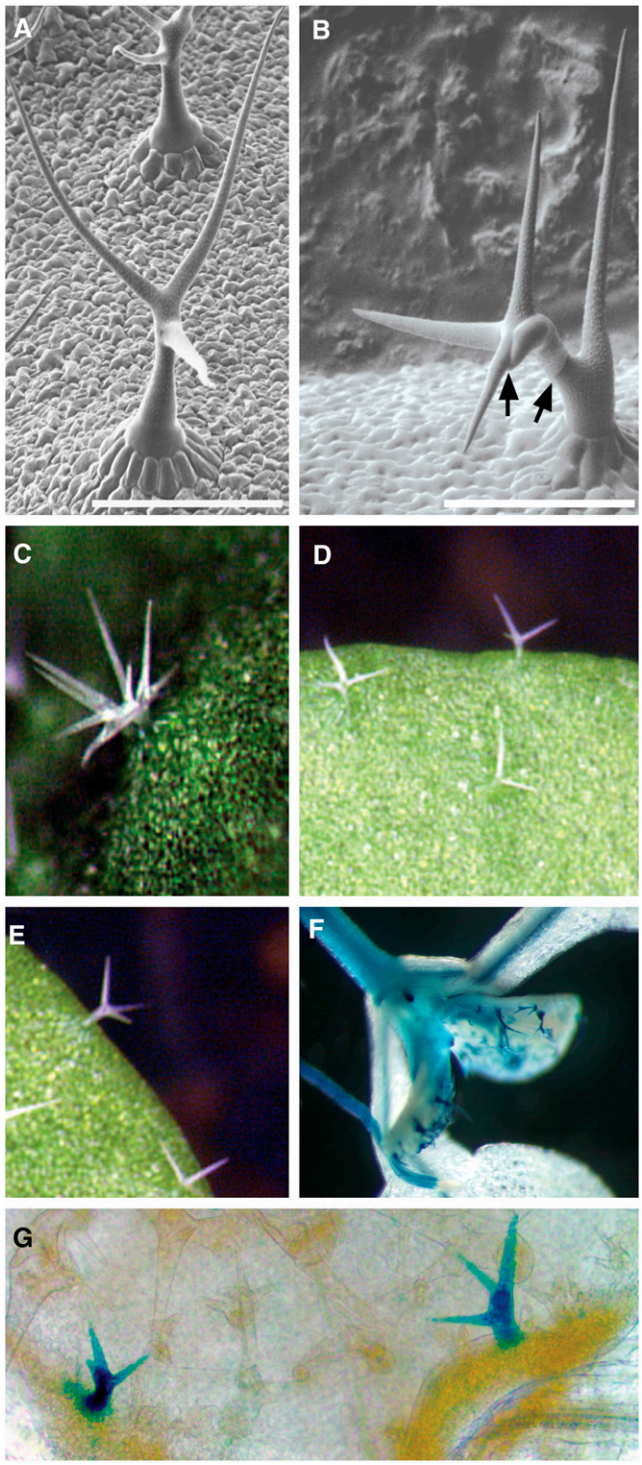

Figure 1. *sim* Loss-of-Function Phenotype.

(A) Scanning electron micrograph of a wild-type trichome.
(B) Scanning electron micrograph of *sim* mutant trichome. Arrows indicate cell junctions.
(C) Light micrograph of *sim* loss-of-function phenotype.
(D) Complementation of *sim* loss-of-function phenotype by *pGL2:SIM*.
(E) Complementation of *sim* loss-of-function phenotype by genomic fragment.
(F) GUS staining pattern of *sim-2* enhancer trap.
(G) pCYCB1;1:GUS expression in *sim* mutant trichomes.
Bars in **(A)** and **(B)** = 200 μm.

to CYCA, CYCE, and CYCD/CDK complexes (Adams et al., 1996; Wohlschlegel et al., 2001). Motif 1 and motif 2 show no obvious similarity to any domains with known functions, although the motif 1 residue P36, mutated to Ser in *sim-3*, is conserved in all of the homologs. SIM (amino acids 26 to 40), SIAMESE-RELATED2 (SMR2) (amino acids 32 to 46), SMR3 (amino acids 33 to 44), Zm SMR2 (amino acids 98 to 109), and *Glycine max* SMR (amino acids 21 to 33) also have PEST domains (PESTfind scores > +6.96) enriched in Pro, Glu, Ser, and Thr residues that often serve as proteolytic signals (Rogers et al., 1986). In addition, SMR1 contains a consensus CDK phosphorylation site (S/TPXK/R) at residues 16-19.

SIM and SMR Yellow Fluorescent Protein Fusions are Nuclear Localized

To determine the subcellular localization of the SIM protein, a 35S:EYFP:SIM (EYFP for enhanced yellow fluorescent protein) gene construct was introduced via biolistic bombardment directly into leaf epidermal cells of *Arabidopsis*. EYFP alone is cytoplasmically localized (Figure 3A), while an EYFP fusion to the transcription factor TGA5 is nuclear localized (Figure 3B). EYFP:SIM expression was detected in nuclei (Figure 3C). The subcellular localizations of the SMRs from *Arabidopsis* were also determined using biolistic bombardment of EYFP fusions into epidermal cells. In all instances, the proteins were localized to nuclei (Figures 3D to 3F).

SIM Interacts with D-Type Cyclins and CDKA;1 in Vivo and Regulates CYCB1;1 Expression

The presence of ICK/KRP-like domains and the Cy motif within the SIM protein suggested that it might associate with cyclins. To test this hypothesis, an ECFP:SIM (ECFP for enhanced cyan fluorescent protein) fusion protein was transiently expressed in the leaf epidermal cells of *Arabidopsis*, along with 35S:EYFP fusion proteins of several different core cell cycle proteins. Subsequently, protein–protein interaction in the cotransformed leaves was analyzed by the acceptor bleaching fluorescence resonance energy transfer (FRET) method. As a positive-control FRET protein pair, the *Arabidopsis* transcription factor TGA5 (At5g06960), whose self-interaction in plants was previously detected by FRET analysis (Cheng et al., 2003), was used. As a negative control, the noninteracting LexA-NLS (a bacteria protein fused to SV40 T-antigen nuclear localization signal) and TGA5 proteins were used (Kato et al., 2002). As an additional negative control, ECFP:SIM was tested for interaction with EYFP:LexA-NLS (Table 1).

We observed that SIM interacted with the D-type cyclins CYCD2;1, CYCD3;2, and CYCD4;1 and with CDKA;1 (Table 1). By contrast, no significant association was observed between SIM and any of the A- or B-type cyclins tested nor with the B-type CDK, CDKB1;1 (Table 1). One homolog, SMR2, was shown to

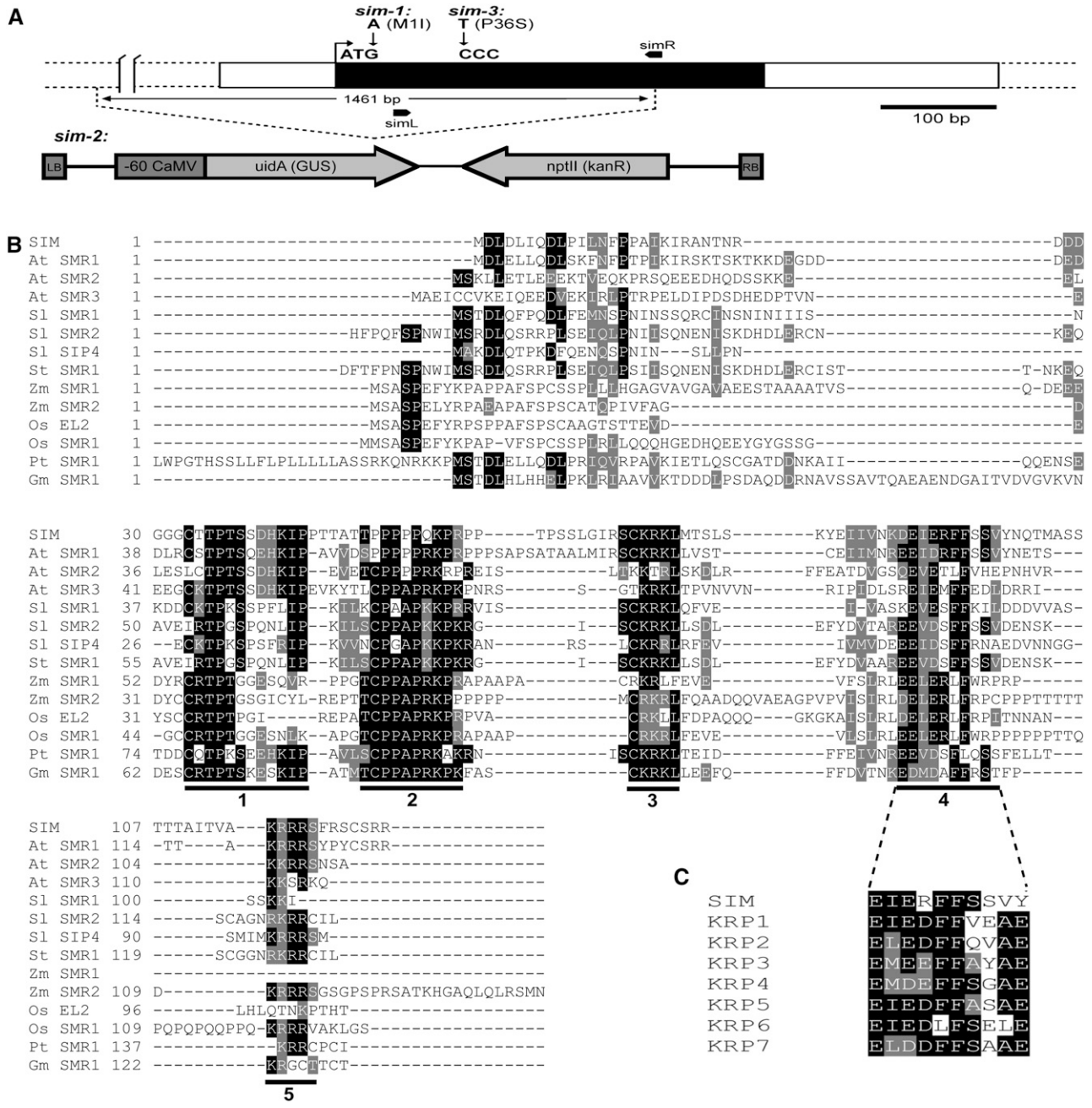

Figure 2. SIM Encodes a Small Protein of Unknown Function Defining a Small Gene Family in *Arabidopsis* and Other Plants.

(A) The *SIM* locus (At5g04470). Sequence changes in mutant alleles are indicated; the *sim-2* gene contains an insertion of the pD991 enhancer trap T-DNA that deletes 1461 bp, including 272 bp of coding sequence and 1189 bp of upstream sequence. simL and simR indicate the primers used for RT-PCR (see Supplemental Figure 1 online).

(B) Alignment of conceptual translation of SIM reading frame and related plant proteins. The regions numbered 1 to 5 denote conserved domains referred to in the text. Sl, *Solanum lycopersicum*; St, *Solanum tuberosum*; Zm, *Zea mays*; Os, *Oryza sativa*; Pt, *Populus tremula*; Gm, *Glycine max*.

(C) Similarity between SIM and D-type cyclin binding domain of ICK/KRPs.

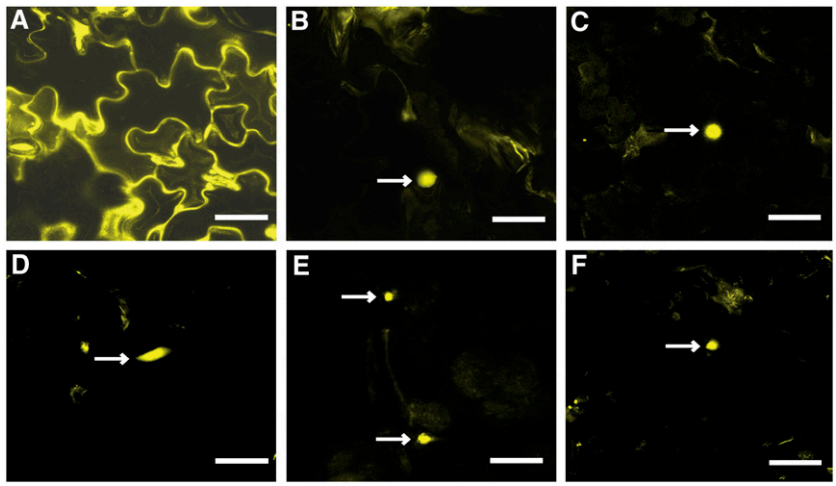

Figure 3. The SIM Family Localizes to the Nucleus.

Expression of EYFP fusion constructs in leaves was examined after introduction by biolistic bombardment of the DNA. EYFP alone **(A)**, cytoplasmically localized; EYFP:TGA5 **(B)**, TGA5 is a nuclear-localized trancription factor (Zhang et al., 1993; Kato et al., 2002); EYFP:SIM **(C)**; EYFP:SMR1 **(D)**; EYFP:SMR2 **(E)**; EYFP:SMR3 **(F)**. Bars = 18.75 μm; arrows indicate nuclei.

interact with CYCD2;1, demonstrating that another SIM family member also associates with a D-type cyclin.

B-type cyclins are required for mitosis and are not normally expressed in wild-type trichomes (Schnittger et al., 2002a). To determine whether B-type cyclins are expressed in *sim* mutant trichomes, a *CYCB1;1*:GUS fusion gene including the *CYCB1;1* promoter and the N-terminal portion of the coding region that encodes the cyclin destruction box was introduced into *sim* plants by crossing. This fusion is thought to mimic the expression pattern of *CYCB1;1* and has been used in other studies to identify G2/M cells (An Colo An-Carmona et al., 1999). We detected GUS expression in a fraction of developing *sim* trichomes (Figure 1G), presumably those in G2/M, suggesting that *CYCB1;1* is ectopically expressed in these cells. No GUS expression was seen in >1000 trichomes of wild-type plants containing this construct.

SIM Family Expression in Plants

The existence of ESTs and our RT-PCR data indicate that *SIM* is expressed. Random amplification of cDNA ends (RACE) and sequencing of RT-PCR–derived cDNA was used to confirm the annotated transcript from public databases. 5′ RACE indicates that the 5′ terminus of the *SIM* transcript lies at chromosomal position 1267369 on chromosome five, 92 bp upstream of the start codon. 3′ RACE indicates that the 3′ terminus of this mRNA lies 217 bp downstream of the stop codon at chromosomal position 1266668. Sequencing of the complete PCR-amplified cDNA confirmed that, as annotated, the gene contains no introns.

Tissue-specific expression of the *SIM* family was analyzed using quantitative RT-PCR. As can be seen in Figure 4A, all family members are expressed to some degree in all tissues examined:

Table 1. SIM Protein–Protein Interactions Determined by FRET

Donor (CFP Fusion)	Acceptor (YFP Fusion)	FRET Efficiency (%)[a]	*n*[b]	P[c]	Interaction?
TGA5	TGA5	17.75	10	<0.0001	Y
TGA5	LexA-NLS	1.10	10	1.000	N
SIM	LexA-NLS	0.79	10	0.9300	N
SIM	CDKB1;1	2.16	10	0.6400	N
SIM	CYCA2;2	2.90	10	0.4300	N
SIM	CYCB2;1	2.01	15	0.5200	N
SIM	CDKA;1	21.91	10	0.0003	Y
SIM	CYCD2;1	14.81	11	0.0003	Y
SIM	CYCD3;2	13.22	10	0.0190	Y
SIM	CYCD4;1	17.70	10	0.0120	Y
SMR2	CYCD2;1	27.43	10	0.0005	Y

[a] The acceptor photobleaching method was used to determine the FRET efficiency (see Methods).
[b] Number of nuclei analyzed.
[c] Student's *t* tests were performed for each data set. P indicates the statistically significant difference between each data set and the negative control values.

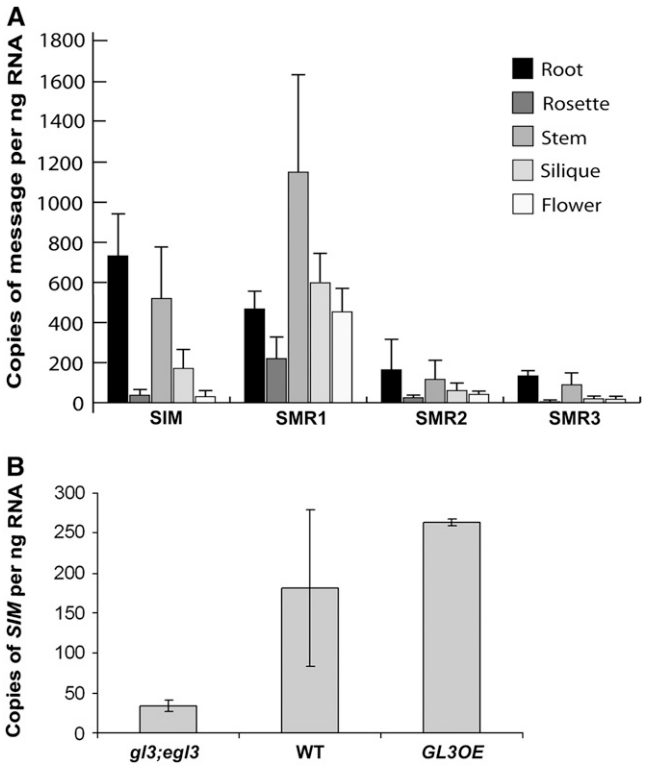

Figure 4. Expression of the *SIM* Gene Family in Various *Arabidopsis* Tissues.

(A) Absolute quantification of *SIM* family transcript levels by quantitative RT-PCR.

(B) Increase of *SIM* transcript levels in response to increasing levels of GL3 function. Expression of *SIM* transcripts in leaves of a *gl3 egl3* line that lacks GL3 function, a Columbia (Col) wild-type line with normal GL3 function, and a line overexpressing *GL3* was compared by quantitative RT-PCR. The values shown represent averages of three separate biological replicates ± SD.

roots, stems, flowers, siliques, and rosettes. Although *sim* mutants have no obvious root phenotype (Walker et al., 2000), SIM expression is particularly strong in root tissue (Figure 4A). While the overall expression pattern of the four genes is quite similar at this whole-tissue level, the relatively high expression level of SMR1 in all inflorescence tissue (stem, unopened flowers, and silique, Figure 4A) is notable. In situ hybridization to shoot apices shows that *SIM* is expressed throughout the shoot apical meristem and in leaf primordia (Figure 5), including developing trichomes (Figure 5A, closed arrows), and in procambial strands and developing vasculature (Figure 5A, open arrows).

As mentioned above, *sim-2* mutants carry an insertion at the SIM locus that includes a GUS enhancer trap. The *sim-2* mutants exhibit GUS expression in both developing and mature trichomes as well as in stipules (Figure 1F). Strong expression is also seen in the vasculature of both the aerial organs and the root (see Supplemental Figure 2 online). The relatively trichome-specific expression of the enhancer trap in developing leaves suggested that a trichome-specific enhancer was located either upstream or downstream of the *SIM* coding region. To test more directly whether some aspects of *SIM* expression were under the control of the trichome developmental pathway, we took advantage of *Arabidopsis* strains expressing various levels of function of the key trichome development transcription factor *GL3* (Payne et al., 2000; Zhang et al., 2003). Plants doubly mutant for *gl3* and its functional duplicate *egl3* lack GL3 function and produce no trichomes, while the *GL3OE* line used here overexpresses the *GL3* transcript and produces a greater number of larger, extra-branched trichomes. Thus, genes that are specifically expressed during trichome development should therefore show little or no expression in *gl3 egl3* mutants and increased expression in the *GL3OE* line. *SIM* transcript levels increase with increasing GL3 function, suggesting that *SIM* expression is at least partially under direct or indirect control of *GL3* (Figure 4B).

Plants Overexpressing SIM Have Greatly Enlarged Cells

To investigate the biological role of SIM in plant development, transgenic plants expressing SIM ectopically from the cauliflower mosaic virus 35S promoter were produced. Six transgenic lines

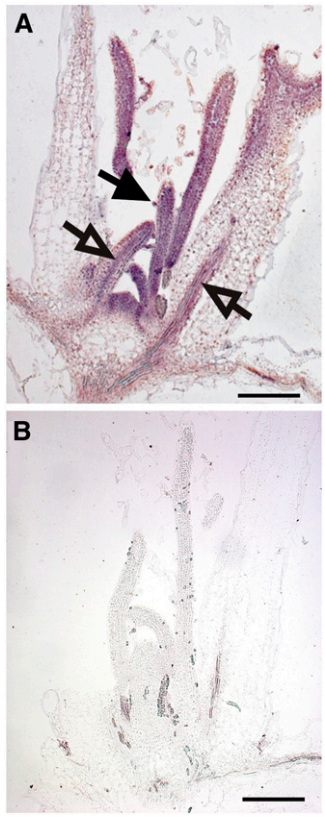

Figure 5. Expression Pattern of *SIM*.

In situ RNA hybridizations to longitudinal sections of the shoot apex probed with DIG-labeled single-stranded antisense *SIM* **(A)** and sense probe of *Ceratopteris richardii* gene of unknown function (**[B]**; accession number CV735270). Closed arrow indicates a developing trichome. Open arrows indicate procambial strands and developing vasculature. Bars = 200 μm.

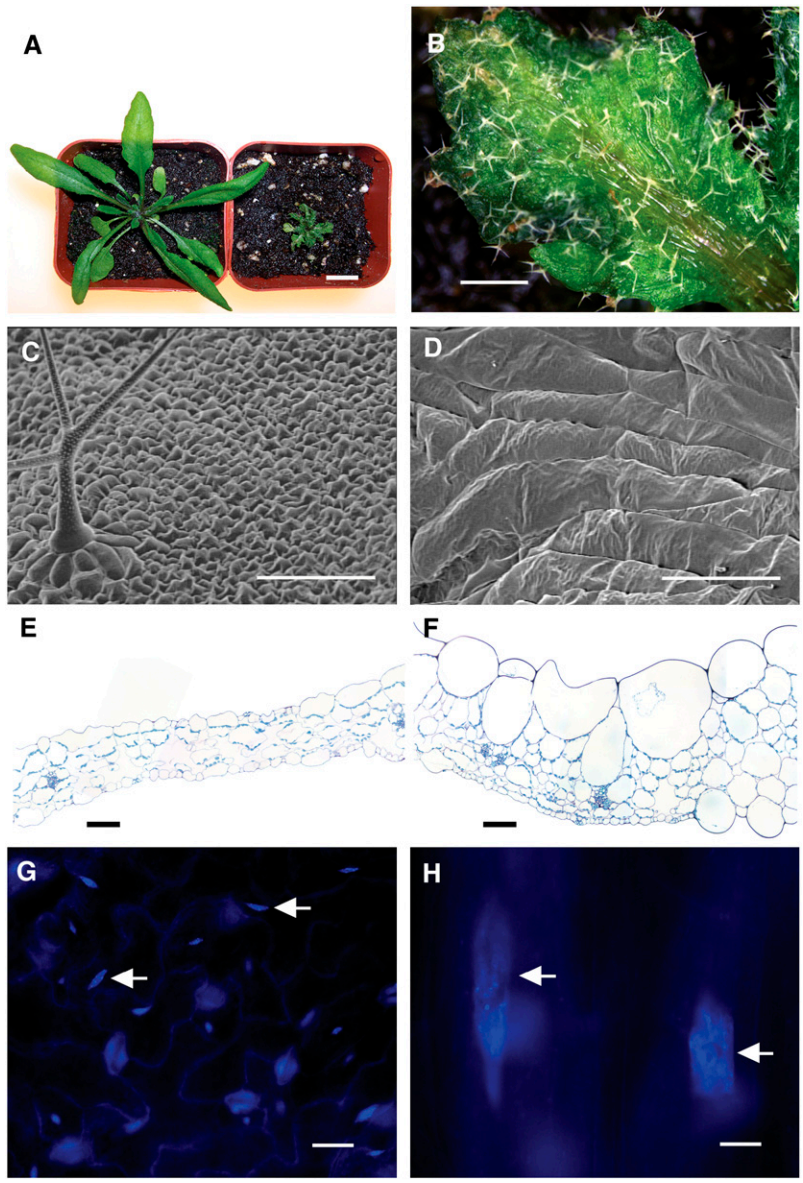

Figure 6. Phenotypic Analysis of SIM-Overexpressing Plants.

(A) Four-week-old wild-type (left) and 35S:SIM (right) plants with inflorescences removed.
(B) Second leaf of 35S:SIM plant shown in **(A)**.
(C) Adaxial epidermal pavement cells of wild-type first leaf.
(D) Adaxial epidermal pavement cells of 35S:SIM first leaf.
(E) Cross section through wild-type first leaf.
(F) Cross section through 35S:SIM first leaf.
(G) DAPI-stained epidermal pavement cell nuclei of wild-type first leaf. Arrows indicate nuclei.
(H) DAPI-stained epidermal pavement cell nuclei of 35S:SIM first leaf. Arrows indicate nuclei.
All analyses were done using 4-week-old wild-type and 35S:SIM plants. Bars = 1 cm in **(A)**, 1 mm in **(B)**, 200 μm in **(C)** and **(D)**, 50 μm in **(E)** and **(F)**, and 22 μm in **(G)** and **(H)**.

containing the *35S:SIM* construct were generated. Plants from five of the six lines showed a similar phenotype. *SIM*-overexpressing plants are dramatically reduced in size compared with the wild type (Figure 6A). Quantitative RT-PCR revealed that these lines express ~50- to 90-fold more *SIM* transcripts than wild-type plants. Although the overall size of the plant is greatly reduced, *35S:SIM* plants (Figures 6B, 6D, and 6F) contain abnormally large epidermal cells in comparison with the wild type (Figures 6C and 6E). As observed by scanning electron microscopy, cell patterning is highly irregular. Cells of *SIM*-overexpressing plants are

highly variable in size and shape, with the largest cells tending to occur in contiguous groups (Figures 6B and 6D). Cross sections reveal that the adaxial epidermis is the most strongly affected cell layer in the leaf, although enlarged subepidermal cells are occasionally observed (Figures 6E and 6F). Trichomes on the leaves of *35S:SIM* plants did not obviously differ from those of the wild type in size or degree of branching, which is not surprising given that expression of *SIM* from the much stronger *GL2* promoter did not affect trichome size or branching. However, when *35S:SIM* was introduced into a *sim-1* background, the results were unexpected. While *35S:SIM*; *sim-1* plants had fewer multicellular trichomes than did *sim-1* plants (43/100 trichomes multicellular in *35S:SIM*; *sim-1* versus 54/100 multicellular in *sim-1*), this difference was not statistically significant ($\chi^2 = 2.42$, $P = 0.120$), indicating that *35S:SIM* complements the mutation only partially if at all. This is in sharp contrast with *pGL2:SIM*, which completely complements *sim-1*.

Insight into this poor complementation of *sim-1* by *35S:SIM* and the cause of the patchy distribution of large cells in *35S:SIM* plants was obtained from transgenic lines expressing N-terminal fluorescent protein:*SIM* fusions from the 35S promoter to test the in vivo functionality of these fusions. Plants expressing these constructs grew more slowly than wild-type plants and produced large epidermal cells (see Supplemental Figure 3 online), suggesting that they were functional in inhibiting mitosis in the leaf epidermis. However, like *35S:SIM*, these *35S:GFP:SIM* (GFP for green fluorescent protein) constructs complemented the *sim-1* mutation only partially (39/96 trichomes multicellular in *35S:GFP:SIM*; *sim-1* versus 58/100 multicellular in *sim-1*), although in this case the complementation was significant ($\chi^2 = 5.92$, $P = 0.015$). Upon examining the GFP expression in multiple independent *35S:GFP:SIM* lines, all plants showed strong expression in nondividing tissues of the root, but expression ceased abruptly at the root-shoot boundary at the base of the hypocotyl (see Supplemental Figure 3 online), and expression was absent in the root tip. Individual *35S:GFP:SIM* plants showed rare and highly variable patterns of expression in leaf tissue, ranging from expression in a single cell type (guard cells, in one instance) to expression in small groups of cells within a leaf. Individual plants derived from the same single-insert-containing *35S:GFP:SIM* line typically showed completely different patterns of reactivation of GFP expression in shoot tissues. Taken together, these observations suggest that there is strong selection against *SIM* expression in dividing tissues of the shoot and root and that in surviving plants, the transgene has been epigenetically silenced in these tissues. Furthermore, these results also suggest an explanation for the low frequency of large endoreplicated cells on the leaves of 35S:SIM plants; these cells may simply represent those few cells that have escaped complete silencing. These results also indicate that N-terminal fluorescent protein:*SIM* fusions are functional.

Plants Overexpressing SIM Undergo Increased Endoreplication

The enlarged epidermal cells in SIM-overexpressing plants contain enlarged nuclei relative to wild-type epidermal cells (Figures 6G and 6H), as expected from the previously described correlation between cell size and nuclear DNA content in *Arabidopsis* leaves (Melaragno et al., 1993). Analysis by flow cytometry confirms that the epidermal pavement cells of 35S:SIM plants undergo extra rounds of endoreplication (Figure 7A), with increased levels of 8C, 16C, and 32C cells clearly detected at 15 and 21 d after sowing (DAS). However, the extremely large epidermal cells observed in Figures 6B, 6D, and 6F represent only a small fraction of the cells in a leaf, even in regions containing a patch of enlarged epidermal cells, and these rare large nuclei might be missed in the flow cytometry experiments.

To estimate the DNA contents of the largest epidermal cells, in situ measurements were made of 4′,6-diamidino-2-phenylindole (DAPI)-stained nuclei of the largest class of adaxial epidermal cells on 35S:SIM plants and compared with equivalent measurements for wild-type adaxial epidermal cells (Figure 7B). In these experiments, the data are presented in terms of relative fluorescence units (RFUs) of DAPI fluorescence detected in the nuclei, but the data have been normalized to the mean value of 4.4C for the DNA content of wild-type Col epidermal nuclei (Melaragno et al., 1993); thus, the RFU values should represent the approximate DNA contents of the nuclei. On this basis, the nuclei of the enlarged epidermal pavement cells of 35S:SIM plants have DNA contents on average of 93.6 ± 45.9C (Figure 7B). However, the 35S:SIM nuclei clearly fall into two major clusters of ~42 and 85 RFU. Because these clusters are almost exactly twofold different in apparent DNA content, and given that in situ DNA contents are complicated by irregular nuclear shapes, background fluorescence, and other factors, a reasonable interpretation is that these two peaks represent nuclei with 32C and 64C DNA contents, respectively. In this case, the largest class of cells would consist primarily of 64C cells, with a substantial number of 32C cells and a few cells of higher C value. This interpretation is broadly consistent with the results of the flow cytometry study, although no 64C cells were detected by flow cytometry. The very largest cells in the adaxial epidermis of these leaves included only a few dozen cells per leaf, and it is possible that the nuclei of these cells were missed in the flow cytometry. However, it should be noted that the plants for flow cytometry and in situ observations were grown under different conditions; plants for flow cytometry were grown on plates for 21 d, while plants for the in situ measurements were grown on soil for 28 d. These differences in growth conditions may explain the differences in the highest ploidy detected.

DISCUSSION

We have isolated and characterized a cell cycle regulator that plays an integral role in controlling the onset of endoreplication in *Arabidopsis*. Loss of SIM function results in multicellular trichomes with decreased levels of endoreplication (Figures 1B and 1C; Walker et al., 2000). We have shown that SIM is encoded by At5g04470, a gene that previously had no known function. Three additional uncharacterized genes from *Arabidopsis*, as well as 10 others from a variety of plant species, have been identified as members of a family of proteins that share five distinct domains with SIM (Figure 2B). Sequence analyses reveal that one of these domains is a putative cyclin binding motif, the Cy motif found in some CDK inhibitors, Rb, and E2F (Adams et al.,

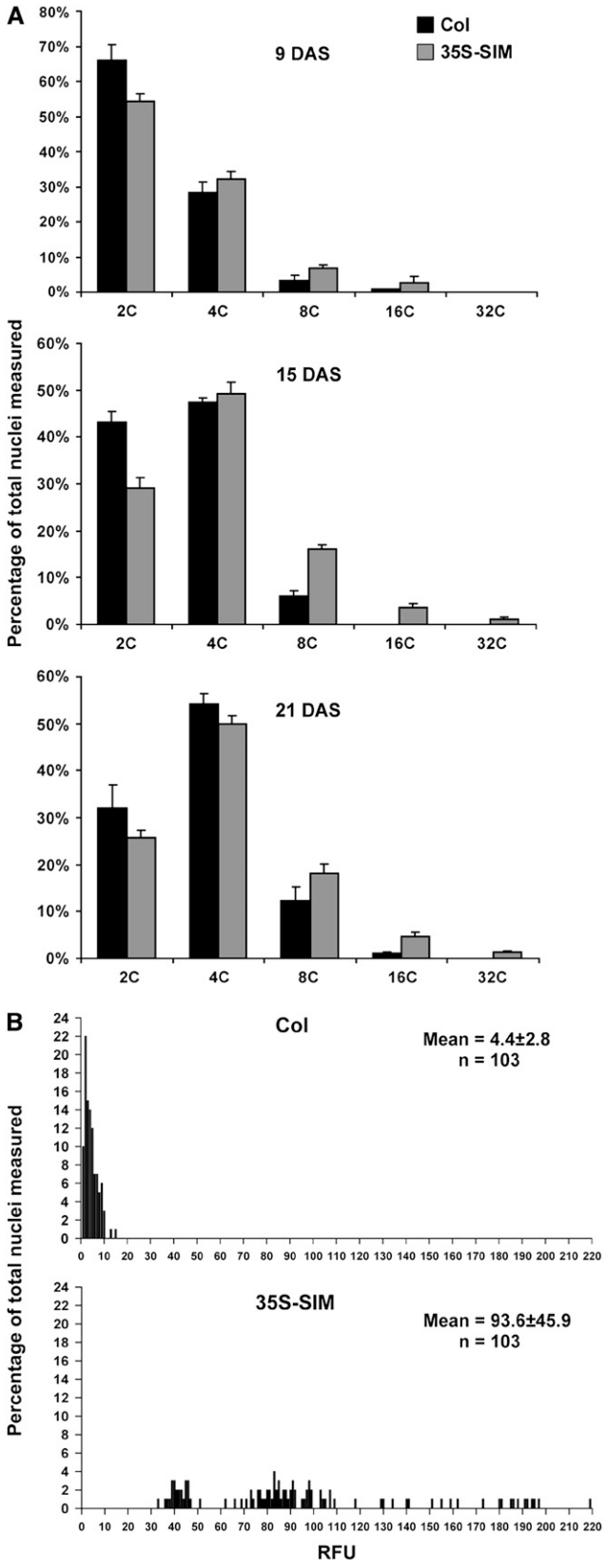

Figure 7. DNA Contents of SIM-Overexpressing Plants.

(A) Ploidy level distribution of the first leaves of wild-type (Col) and 35S:SIM plants at 9, 15, and 21 DAS as measured by flow cytometry. The indicated values are means ± SD ($n = 3$ to 5).

(B) Relative DNA contents of DAPI-stained epidermal pavement cell nuclei of wild-type (Col) and 35S:SIM enlarged cells of plants at 28 DAS. The degree of fluorescence is expressed as RFUs normalized to the mean fluorescence of Col. These RFU values have been adjusted to be comparable to published C values (see Methods), but they should only be interpreted as relative comparisons, not as measurements of absolute DNA contents.

1996; Wohlschlegel et al., 2001). Another motif is shared with the CDK-inhibitory ICK/KRP proteins, which are known to bind to D-type cyclins (Wang et al., 1998; De Veylder et al., 2001). We demonstrate that EYFP fusions of SIM and its *Arabidopsis* homologs are localized to the nucleus (Figures 3C to 3F) and are expressed throughout the plant, including meristems, leaf primordia, and trichomes (Figures 4A and 5A).

Overexpression of SIM results in severely dwarfed plants, with varying degrees of enlarged cells having highly endoreplicated nuclei (Figures 6 and 7). Together with the loss-of-function phenotype, this gain-of-function phenotype supports a role for SIM in inhibiting mitosis, thereby promoting endoreplication. Our in vivo FRET experiments (Table 1) suggest that SIM interacts with one or more CYCD/CDKA;1 complexes but does not interact with B-type mitotic cyclins or with mitosis-specific CDKB-containing complexes. This result is consistent with the observation that *sim* mutants express a *CYCB1;1:GUS* reporter gene (Figure 1G) and also express *CYCB1;2* transcripts (Schnittger et al., 2002a). These results indicate that *SIM* acts upstream of the G2 induction of *CYCB* expression.

The observation that SIM, a negative regulator of mitosis in endoreplicating trichomes, may interact with CYCD/CDK complexes was initially surprising. CYCD/CDK complexes are typically considered to function at the G1/S transition, promoting entry into S-phase (De Veylder et al., 2003; Dewitte and Murray, 2003; Inzé, 2005; Menges et al., 2006). However, there are several lines of evidence that are consistent with the hypothesis that SIM functions primarily or exclusively via its interactions with CYCD/CDK complexes. First, overexpression of a D-type cyclin in trichomes causes production of multicellular trichomes, which phenocopies the *sim* phenotype (Schnittger et al., 2002b). In *sim* mutants, D-cyclin overexpression produces an even stronger phenotype, consistent with SIM acting as a negative regulator of D-type cyclins. Second, the *sim* mutant phenotype is rescued when *ICK1/KRP1*, a CDK inhibitor known to interact with D-type cyclins, is ectopically expressed in trichomes (Weinl et al., 2005). Finally, like the ICK/KRP proteins, SIM is a small, nuclear-localized protein, and SIM shares one short motif with the ICK/KRP family of proteins (Figure 2C). Considering all of this evidence together, it is likely that SIM functions as a CDK inhibitor by interacting with CYCD/CDK complexes.

Our work and the work of Schnittger et al. (2002b) indicate that in addition to their known role at the G1/S transition, CYCD/CDKA complexes can promote mitosis in developing trichomes. In contrast with this observation, Murray and colleagues have shown that overexpression of *CYCD3;1* from the *35S* promoter leads to a

decrease in cells in G1 and an increase in cells in G2 as well as an extended G2 phase and a delay in CYCB activation (Dewitte et al., 2003; Menges et al., 2006). These observations are consistent with a specific role of CYCD3;1 at the G1/S transition and do not support a role for this cyclin in promoting mitosis. One possible explanation is that endoreplicating trichome cells lack a cell cycle checkpoint that normally prevents D-cyclins from promoting mitosis, and SIM is needed to prevent mitosis. Alternatively, the in vivo target of SIM may be a specific CYCD/CDK complex that can play a role in promoting mitosis. *Arabidopsis* has 10 *CYCD* genes, and only a few have been functionally examined. It is not known which *CYCD* genes are expressed in developing trichomes, although *CYCD3;1* is not (Schnittger et al., 2002b). It should be noted that while the acceptor photobleaching FRET method is unlikely to produce false positives, it is possible that true interactions might not be detected either due to the specific geometry of the complexes involved or to a low signal-to-noise ratio. Thus, we cannot rule out the possibility that SIM might interact with additional complexes among those tested.

The observation that *SIM* transcript levels show some degree of dependence on expression of the trichome developmental regulator *GL3* (Figure 4B) suggests that regulation of *SIM* expression levels may play a role in the transition to endoreplication during trichome development. However, *SIM* transcript expression by itself is not sufficient to block mitosis; *SIM* transcripts are detected throughout the meristem and young leaf primordia (Figure 5A), yet these cells continue to divide. Also, the effect of SIM overexpression is tissue specific, with much larger cells occurring in the adaxial epidermis of leaves than in the abaxial epidermis or mesophyll (Figure 6F). These observations suggest that SIM expression is under posttranscriptional control, like many other cell cycle components, or that SIM function requires other trichome-specific components. Alternatively, these tissues may lack some activator or cofactor required for SIM function.

SIM is expressed in a wide variety of tissues (Figures 4A and 5A), yet the *sim* mutant phenotype has been detected only in trichome and hypocotyl cells (Walker et al., 2000). The existence of three *Arabidopsis* SIM homologs, the *SMR* genes, suggests that the *SIM* may play additional roles beyond those detected in *sim* homozygotes that are concealed by functional overlap with the other family members. *SIM* is particularly strongly expressed in roots (Figure 4A) and in procambial cells and developing vasculature (Figure 5A) and may play a role in root or vascular development. Further insight into the potential role of *SIM* and the *SMR* genes in the root comes from the cell-type-specific microarray expression study of Birnbaum et al. (2003). In this study, transcripts of *SIM*, *SMR1*, and *SMR3* were detected in all tissue layers of the root, and consistent with our results in Figure 4A, *SIM* expression is the strongest, and *SMR3* is much more weakly expressed than the other two genes. In the Birnbaum et al. (2003) study, expression was also examined in three developmental stages along the root axis. Stage one contains the root tip and would be expected to have the highest proportion of dividing cells; this assumption is supported by the relative transcript levels of mitotic cyclins, which were highest in this stage. Stage two included cells that were dividing less frequently and are beginning to differentiate, and stage three contained the zone of rapid cell elongation. Expression of *SIM*, *SMR1*, and *SMR3* is much lower in stage one than in the other stages, and both *SIM* and *SMR1* exhibit their highest expression level at stage two. Expression of *SMR3* steadily increases from stage one, the root tip, to stage three, the expanding cells. This pattern of expression of *SIM* and its paralogs is consistent with a role in reduced division rates concomitant with cell differentiation and the onset of endoreplication.

One clue to other potential functions of *SIM* and its homologs is that a tomato (*Solanum lycopersicum*) homolog of *SIM* has been implicated in a signaling pathway involved in inflorescence development. *SELF-PRUNING INTERACTING PROTEIN4* (*SIP4*; shown as Sl SIP4 in Figure 2B) was isolated in a yeast two-hybrid screen using the tomato *SELF-PRUNING* (*SP*) protein as bait (Pnueli et al., 2001). *SP* is the functional homolog of *TERMINAL FLOWER* (*TFL*) in *Arabidopsis* and *CENTRORADIALIS* (*CEN*) in *Antirrhinum majus* (Pnueli et al., 1998). Members of the TFL/SP/CEN family control inflorescence determinacy and architecture (Shannon and Meeks-Wagner, 1991; Alvarez et al., 1992; Bradley et al., 1997; Pnueli et al., 1998). These genes encode members of a plant family of proteins related to the animal phosphatidylethanolamine binding proteins, signaling proteins that appear to act via the kinase Raf1 in animals. A Ser/Thr kinase that was isolated in this same yeast two-hybrid screen was shown to phosphorylate SIP4 on a Ser residue that is conserved in SIM and several other homologs (Pnueli et al., 2001; final S residue in motif 5 in Figure 2B). One of the first events classically observed in the transition to flowering is an increase in mitosis in the meristem (Steeves and Sussex, 1989), and it is tempting to speculate that other members of the *SIM* gene family could be involved in regulating mitotic cycling during this developmental transition.

Our results indicate that *SIM* encodes a cell cycle regulator that plays a key role in the establishment of endoreplication during trichome development. The SIM protein appears to act by regulating D-type cyclin-containing CDK complexes. Plant genomes have significantly larger gene families for most cell cycle components, suggesting that the plant cell cycle may have additional complexity (Vandepoele et al., 2002). For example, there are 10 *CYCD* genes in the *Arabidopsis* genome, whereas in mammals there are only three. Study of *SIM* and its homologs may give additional insights into the diversity of plant cell cycle responses and their integration with development, in addition to giving insights into the establishment of endoreplication.

METHODS

Isolation of *SIM*

The *sim-2* allele, generated by insertional mutagenesis with the T-DNA pD991, originally segregated two inserts. Linkage between a single T-DNA insert and the *sim* phenotype and kanamycin resistance was established. The T-DNA right border junction was recovered from genomic DNA by an adaptor PCR method (Siebert et al., 1995) using pD991-specific primers available on the Jack lab website (www.dartmouth.edu/~tjack/index.html).

To pinpoint the position of the pD991 insert in entirety, PCR reactions with various combinations of primers in the At5g04470 region were performed. Failure to amplify a region in *sim-2* DNA was indication of the insert; wild-type DNA was used as a positive control for the primers. Finally, the exact position of the left border of pD991 was identified by sequencing a DNA fragment that was PCR amplified using a primer specific for the left border, oligo 156 (5′-CCCTATAAATACGACGGATCG-3′),

and primer specific for a region of *sim-2* that is able to be amplified, T32m21-23337L (5′-ACATACTTGTGCATGTGCCTCTCGC-3′).

For molecular complementation analysis, the genomic coding sequence of *At5g04470*, 2870 bp of upstream sequence, and 250 bp downstream sequence was PCR amplified from the BAC clone T32M21 using the primers simwhole3500 L (5′-AGCATAAACA-CCAAGAGAGG-ACC-3′) and simwhole R (5′-ATACTTGTGCATGTGCCTCTCCT-3′). This fragment was cloned into the pCR2.1 vector (Invitrogen) by TOPO cloning (Invitrogen) to create pSIM3500. The pSIM3500 insert was subcloned as a *Bam*HI-*Xho*I fragment into these sites of the binary vector pBIN19 (Bevan, 1984) to create pSIM3500Bin, which was used to complement the *sim* phenotype.

For RT-PCR analysis of At5g04470 expression in Wassilewskija and *sim-2* plants, RNA was harvested from the shoot tissue of 3-week-old Wassilewskija and *sim-2* plants using the Plant RNeasy kit (Qiagen) following the manufacturer's instructions. cDNA was synthesized from this RNA using the Omniscript RT kit (Qiagen). The presence of the *SIM* transcript was measured by PCR amplification using this cDNA as template and the primers simL (5′-AGATCTGCCCATCTTGAATTTCCC-3′) and simR (5′-GCTCGATCTCATCTTTGTTGACGAT-3′) to assess the presence of the *SIM* transcript and the primers HIS4 L (5′-TCGTG-GAAAGGGAGGAAAAGGT-3′) and HIS4 R (5′-CTAGCGTGCTCGGTGT-AAGTGAC-3′) to assess the presence of a control gene, *HISTONE H4*.

Expression Analysis

The *uidA* (GUS) expression in *sim-2* plants was visualized using methods described previously (Larkin et al., 1996). In situ RNA hybridization was essentially performed as described previously (Larkin et al., 1993). DIG-labeled, single-stranded RNA probes were synthesized from PCR-derived template containing an appropriately positioned T7 promoter to produce a sense or antisense probe. A DIG-labeled, single-stranded sense strand of a *Ceratopteris richardii* (C-fern) gene of unknown function (accession number CV735270) was used as a negative control.

For quantitative RT-PCR, RNA was extracted from various organs of wild-type (Col) plants to assess the expression of *SIM* and its homologs in these tissues using the Plant RNeasy kit (Qiagen) and treated with DNase using a DNase kit (Qiagen) following the manufacturer's instructions. cDNA was synthesized from the RNA harvested from each tissue using an Omniscript RT kit (Qiagen). The absolute transcript levels for *SIM* and its homologs was assessed using the TaqMan method of quantitative RT-PCR (Gibson et al., 1996). A primer pair and FAM/BHQ1 probe was acquired for each transcript of interest. The PCR amplification product of each primer pair was quantified using a spectrophotometer and diluted to make a five-point standard curve for each gene. Each point of the standard curve and each cDNA reaction were run in triplicate. Each point on the graph in Figure 4 is the average of the nine separate reactions run for each gene in each tissue type (three replicates of each of the three biological replicates per tissue).

Generation of Transgenic Lines and Growth Conditions

The full-length *SIM*, At1g08180, At3g10525, and At5g02420 coding regions were PCR amplified from the BAC clones T32M21, T23G18, F13M14, and T22F11, respectively, in two-stage PCR reaction and inserted into the GATEWAY vector pDONR221 (Invitrogen) by attB recombination following the manufacturer's protocol. Error-free entry clones were confirmed by sequence analysis before recombination into the following relevant destination vectors: overexpression, pK2GW7 (www.vib.be); YFP fusions, pDuEX-An_1 (N. Kato, unpublished data); and CFP fusions, pDuEX-Dn_2 (N. Kato, unpublished data). The resulting plasmids were introduced into *Agrobacterium tumefaciens* by transformation and subsequently into plants (ecotype Col) via the floral dip method (Clough and Bent, 1998). Transgenic plants were selected on kanamycin-containing medium and later transferred to soil. Plants were grown as previously described (Larkin et al., 1999). For YFP and CFP gene fusions, vectors were directly introduced to *Arabidopsis thaliana* leaves via particle bombardment using a PDS-1000/He biolistic particle delivery system (Bio-Rad), incubated overnight in water at room temperature with constant shaking, and visualized on a Leica TCS SP2 spectral confocal microscope. Scanning electron microscopy was performed as previously described (Larkin et al., 1999).

Nuclear DNA Measurements

DNA contents were measured as previously described (Walker et al., 2000), with the exceptions that nuclei were observed using a ×20 objective lens, and DNA values were normalized to reported wild-type epidermal cell nuclei values (Melaragno et al., 1993). Flow cytometric analysis was performed as previously described (Verkest et al., 2005).

FRET Analysis

FRET efficiencies of protein pairs in *Arabidopsis* leaf epidermal cells were measured by an acceptor bleaching method (Szczesna-Skorupa et al., 2003). In this method, a protein pair is fused to CFP and YFP. YFP is selectively photobleached with a high intensity of the excitation laser, and changes of CFP intensity before and after the YFP photobleaching are monitored. If the protein pair interacts, CFP intensity will increase after YFP photobleaching due to a loss of the FRET. If the protein pair does not interact, CFP intensity will not change. Hence, the FRET efficiency in this method is quantified as:

$$\mathrm{FRET}_{\mathrm{eff}} = (\mathrm{D}_{\mathrm{post}} - \mathrm{D}_{\mathrm{pre}})/\mathrm{D}_{\mathrm{post}},$$

where $\mathrm{FRET}_{\mathrm{eff}}$ is FRET efficiency, $\mathrm{D}_{\mathrm{post}}$ is the fluorescence intensity of the donor (CFP) after acceptor (YFP) photobleaching, and $\mathrm{D}_{\mathrm{pre}}$ is the fluorescence intensity of the donor before acceptor photobleaching. FRET efficiency is considered positive when $\mathrm{D}_{\mathrm{post}} > \mathrm{D}_{\mathrm{pre}}$.

Arabidopsis leaves that transiently express fusion proteins were observed with a Leica TCS SP2 spectral confocal microscope with a ×40, 1.25–numerical aperture oil immersion objective lens and a double 458/514-nm dichroic mirror. The argon laser line of 458 nm was used to excite ECFP (photomultiplier tube window: 465 to 515 nm) and the 514-nm line to excite EYFP (photomultiplier tube window: 525 to 570 nm). To increase photon fluxes, a pinhole size of the confocal microscope was increased to 600 mm from the default size of 81.39 mm (Airy 1). The image was zoomed 3.5- to 5-fold, and the nucleus region where both ECFP and EYFP were detected was selectively bleached with the 514-nm line at 100% laser intensity. Three to ten percent of the 514-nm laser intensity was used to monitor changes of EYFP fluorescence intensity during the bleach. The nucleus region was bleached 20 times in ~2 min, and the ECFP intensity in the bleached region was measured before and after the EYFP bleaching. The FRET Wizard program in the Leica confocal microscope software (LCS 2.61.1537) was used to set experimental conditions and calculate FRET efficiencies.

Accession Numbers

Sequence data from this article can be found in the GenBank/EMBL data libraries under the following accession numbers: SIM (At5g04470), CAB85553; SMR1 (At3g10525), BAC42937; SMR2 (At1g08180), AAF18255; SMR3 (At5g02420), CAB85979; *Solanum lycopersicum* SMR1, AI780963; *S. lycopersicum* SMR2, AW931119; *S. lycopersicum* SIP4, AAG43410; *S. tuberosum* SMR1, BM110486; *Zea mays* SMR1, AZM4_61016; *Z. mays* SMR2, AZM4_26293; *Oryza sativa* EL2, T03676; *O. sativa* SMR1, AAK20052; *Populus tremula* SMR1, BU815024; and

Glycine max SMR1, AW704877. All of these accession numbers are from the National Center for Biotechnology Information database, with the exception of *Z. mays* SMR1 and *Z. mays* SMR2, which are from The Institute for Genomic Research.

Supplemental Data

The following materials are available in the online version of this article.

Supplemental Figure 1. *At5g04470* Expression in *sim-2* Plants.

Supplemental Figure 2. GUS Expression in *sim-2* Plants.

Supplemental Figure 3. Expression of the 35S:GFP:SIM Fusion Protein.

ACKNOWLEDGMENTS

We thank Ying Xiao, David Burk, and Margaret C. Henk of the Socolofsky Microscopy Center for assistance with microscopy and M. David Marks (University of Minnesota, St. Paul, MN) for the *sim-3* allele. We thank Juan-Antonio Torres-Acosta for materials and helpful discussions and Sara Maes, Els Van Der Schureen, Steve Pollock, and Alice Simmons for technical assistance. We also thank Kristen Prufer and James Moroney for critical comments on the manuscript. This work was supported by National Science Foundation Grant IOB 0444560 to J.C.L., National Science Foundation Grant DBI 0115684 to D.G.O., and the Louisiana Governor's Biotechnology Initiative. This publication was also made possible by National Institutes of Health Grant P20 RR16456 from the Biomedical Research Infrastructure Networks Program of the National Center for Research Resources. Its contents are solely the responsibility of authors and do not necessarily represent the official views of the National Institutes of Health.

Received June 13, 2006; revised August 15, 2006; accepted October 26, 2006; published November 10, 2006.

REFERENCES

Adams, P., Sellers, W., Sharma, S., Wu, A., Nalin, C., and Kaelin, W. (1996). Identification of a cyclin-cdk2 recognition motif present in substrates and p21-like cyclin-dependent kinase inhibitors. Mol. Cell. Biol. **16,** 6623–6633.

Alvarez, J., Guli, C.L., Yu, X.H., and Smyth, D.R. (1992). Terminal Flower: A gene affecting inflorescence development in *Arabidopsis thaliana*. Plant J. **2,** 103–116.

An Colo An-Carmona, A., You, R., Haimovitch-Gal, Y., and Doerner, P. (1999). Spatio-temporal analysis of mitotic activity with a labile cyclin:GUS fusion protein. Plant J. **20,** 503–508.

Barlow, P. (1978). Endopolyploidy: Towards an understanding of its biological significance. Acta Biotheor. **27,** 1–18.

Bevan, M. (1984). Binary Agrobacterium vectors for plant transformation. Nucleic Acids Res. **12,** 8711–8721.

Birnbaum, K., Sasha, D.E., Wang, J.Y., Jung, J.W., Lambert, G.M., Galbraith, D.W., and Benfey, P.N. (2003). A gene expression map of the *Arabidopsis* root. Science **302,** 1956–1960.

Bradley, D., Ratcliffe, O.J., Vincent, C., Carpenter, R., and Coen, E.S. (1997). Inflorescence commitment and architecture in Arabidopsis. Science **275,** 80–83.

Campisi, L., Yang, Y., Yi, Y., Heilig, E., Herman, B., Cassista, A.J., Allen, D.W., Xiang, H., and Jack, T. (1999). Generation of enhancer trap lines in Arabidopsis and characterization of expression patterns in the inflorescence. Plant J. **17,** 699–707.

Cheng, Y., Kato, N., Wang, W., Li, J., and Chen, X. (2003). Two RNA binding proteins, HEN4 and HUA1, act in the processing of *AGAMOUS* pre-mRNA in *Arabidopsis thaliana*. Dev. Cell **4,** 53–66.

Clough, S.J., and Bent, A.F. (1998). Floral dip: A simplified method for Agrobacterium-mediated transformation of *Arabidopsis thaliana*. Plant J. **16,** 735–743.

De Veylder, L., Beeckman, T., Beemster, G.T.S., Krols, L., Terras, P., Landrieu, I., Van der Schueren, E., Maes, S., Naudts, M., and Inzé, D. (2001). Functional analysis of cyclin-dependent kinase inhibitors of Arabidopsis. Plant Cell **13,** 1653–1667.

De Veylder, L., Joubes, J., and Inzé, D. (2003). Plant cell cycle transitions. Curr. Opin. Plant Biol. **6,** 536–543.

Dewitte, W., and Murray, J.A.H. (2003). The plant cell cycle. Annu. Rev. Plant Biol. **54,** 235–264.

Dewitte, W., Riou-Khamlichi, C., Scofield, S., Healy, J.M.S., Jacquard, A., Kilby, N.J., and Murray, J.A.H. (2003). Altered cell cycle distribution, hyperplasia, and inhibited differentiation in Arabidopsis caused by the D-type cyclin CYCD3. Plant Cell **15,** 79–92.

Edgar, B.A., and Orr-Weaver, T.L. (2001). Endoreplication cell cycles: More for less. Cell **105,** 297–306.

El Refy, A., Zekraoui, L., Valay, J.G., Bechtold, N., Brown, S., Hulskamp, M., Herzog, M., and Bonneville, J.M. (2003). The Arabidopsis KAKTUS gene encodes a HECT protein and controls the number of endoreduplication cycles. Mol. Genet. Genomics **270,** 403–414.

Gibson, U.E., Heid, C.A., and Williams, P.M. (1996). A novel method for real time quantitative RT-PCR. Genome Res. **6,** 995–1001.

Grafi, G., and Larkins, B.A. (1995). Endoreduplication in maize endosperm: Involvement of M phase-promoting factor inhibition and induction of S phase-related kinases. Science **269,** 1262–1264.

Hülskamp, M., Misra, S., and Jurgens, G. (1994). Genetic dissection of trichome cell development in Arabidopsis. Cell **76,** 555–566.

Inzé, D. (2005). Green light for the cell cycle. EMBO J. **24,** 657–662.

Kato, N., Pontier, D., and Lam, E. (2002). Spectral profiling for the simultaneous observation of four distinct fluorescent proteins and detection of protein-protein interaction via fluorescence resonance energy transfer in tobacco leaf nuclei. Plant Physiol. **129,** 931–942.

Kowles, R.V., and Phillips, R.L. (1985). DNA amplification patterns in maize endosperm nuclei during kernel development. Proc. Natl. Acad. Sci. USA **82,** 7010–7014.

Larkin, J.C., Oppenheimer, D.G., Pollock, S., and Marks, M.D. (1993). Arabidopsis glabrous1 gene requires downstream sequences for function. Plant Cell **5,** 1739–1748.

Larkin, J.C., Walker, J.D., Bolognesi-Winfield, A.C., Gray, J.C., and Walker, A.R. (1999). Allele-specific interactions between ttg and gl1 during trichome development in *Arabidopsis thaliana*. Genetics **151,** 1591–1604.

Larkin, J.C., Young, N., Prigge, M., and Marks, M.D. (1996). The control of trichome spacing and number in Arabidopsis. Development **122,** 997–1005.

Larkins, B.A., Dilkes, B.P., Dante, R.A., Coelho, C.M., Woo, Y.M., and Liu, Y. (2001). Investigating the hows and whys of DNA endoreduplication. J. Exp. Bot. **52,** 183–192.

Melaragno, J.E., Mehrotra, B., and Coleman, A.W. (1993). Relationship between endopolyploidy and cell size in epidermal tissue of Arabidopsis. Plant Cell **5,** 1661–1668.

Menges, M., Samland, A., Planchais, S., and Murray, J. (2006). The D-type cyclin CYCD3;1 is limiting for the G1-to-S-phase transition in Arabidopsis. Plant Cell **18,** 893–906.

Nagl, W. (1976). DNA endoreduplication and polyteny understood as evolutionary strategies. Nature **261,** 614–615.

Nakai, T., Kato, K., Shinmyo, A., and Sekine, M. (2006). Arabidopsis KRPs have distinct inhibitory activity toward cyclin D2-associated kinases, including plant-specific B-type cyclin-dependent kinase. FEBS Lett. **580,** 336–340.

Payne, C.T., Zhang, F., and Lloyd, A.M. (2000). GL3 encodes a bHLH protein that regulates trichome development in Arabidopsis through interaction with GL1 and TTG1. Genetics **156,** 1349–1362.

Perazza, D., Herzog, M., Hulskamp, M., Brown, S., Dorne, A.M., and Bonneville, J.M. (1999). Trichome cell growth in *Arabidopsis thaliana* can be derepressed by mutations in at least five genes. Genetics **152,** 461–476.

Pettko-Szandtner, A., Meszaros, T., Horvath, G.V., Bako, L., Csordas-Toth, E., Blastyak, A., Zhiponova, M., Miskolczi, P., and Dudits, D. (2006). Activation of an alfalfa cyclin-dependent kinase inhibitor by calmodulin-like domain protein kinase. Plant J. **4,** 111–123.

Pnueli, L., Carmel-Goren, L., Hareven, D., Gutfinger, T., Alvarez, J., Ganal, M., Zamir, D., and Lifschitz, E. (1998). The SELF-PRUNING gene of tomato regulates vegetative to reproductive switching of sympodial meristems and is the ortholog of CEN and TFL1. Development **125,** 1979–1989.

Pnueli, L., Gutfinger, T., Hareven, D., Ben-Naim, O., Ron, N., Adir, N., and Lifschitz, E. (2001). Tomato SP-interacting proteins define a conserved signaling system that regulates shoot architecture and flowering. Plant Cell **13,** 2687–2702.

Rogers, S., Wells, R., and Rechsteiner, M. (1986). Amino acid sequences common to rapidly degraded proteins: The PEST hypothesis. Science **234,** 364–368.

Schnittger, A., Schobinger, U., Bouyer, D., Weinl, C., Stierhof, Y.D., and Hulskamp, M. (2002b). Ectopic D-type cyclin expression induces not only DNA replication but also cell division in Arabidopsis trichomes. Proc. Natl. Acad. Sci. USA **99,** 6410–6415.

Schnittger, A., Schobinger, U., Stierhof, Y.D., and Hulskamp, M. (2002a). Ectopic B-type cyclin expression induces mitotic cycles in endoreduplicating Arabidopsis trichomes. Curr. Biol. **12,** 415–420.

Shannon, S., and Meeks-Wagner, D.R. (1991). A mutation in the Arabidopsis TFL1 gene affects inflorescence meristem development. Plant Cell **3,** 877–892.

Siebert, P.D., Chenchik, A., Kellogg, D.E., Lukyanov, K.A., and Lukyanov, S.A. (1995). An improved PCR method for walking in uncloned genomic DNA. Nucleic Acids Res. **23,** 1087–1088.

Steeves, T., and Sussex, I. (1989). Patterns in Plant Development, 2nd ed. (Cambridge, UK: Cambridge University Press).

Szczesna-Skorupa, E., Mallah, B., and Kemper, B. (2003). Fluorescence resonance energy transfer analysis of cytochromes P4502C2 and 2E1 molecular interactions in living cells. J. Biol. Chem. **278,** 31269–31276.

Vandepoele, K., Raes, J., De Veylder, L., Rouze, P., Rombauts, S., and Inzé, D. (2002). Genome-wide analysis of core cell cycle genes in Arabidopsis. Plant Cell **14,** 903–916.

Van't Hof, J. (1999). Increased nuclear DNA content in developing cotton fiber cells. Am. J. Bot. **86,** 776–779.

Verkest, A., Manes, C.L.D., Vercruysse, S., Maes, S., Van der Schueren, E., Beeckman, T., Genschik, P., Kuiper, M., Inzé, D., and De Veylder, L. (2005). The cyclin-dependent kinase inhibitor KRP2 controls the onset of the endoreduplication cycle during Arabidopsis leaf development through inhibition of mitotic CDKA;1 kinase complexes. Plant Cell **17,** 1723–1736.

Vlieghe, K., Boudolf, V., Beemster, G.T.S., Maes, S., Magyar, Z., Atanassova, A., Engler, J.D., De Groodt, R., Inzé, D., and De Veylder, L. (2005). The DP-E2F-like gene DEL1 controls the endocycle in *Arabidopsis thaliana*. Curr. Biol. **15,** 59–63.

Walker, J., Oppenheimer, D., Concienne, J., and Larkin, J. (2000). SIAMESE, a gene controlling the endoreduplication cell cycle in *Arabidopsis thaliana* trichomes. Development **127,** 3931–3940.

Wang, H., Fowke, L.C., and Crosby, W.L. (1997). A plant cyclin-dependent kinase inhibitor gene. Nature **386,** 451–452.

Wang, H., Qi, Q., Schorr, P., Cutler, A.J., Crosby, W.L., and Fowke, L.C. (1998). ICK1, a cyclin-dependent protein kinase inhibitor from *Arabidopsis thaliana* interacts with both Cdc2a and CycD3, and its expression is induced by abscisic acid. Plant J. **15,** 501–510.

Wang, H., Zhou, Y.M., Gilmer, S., Whitwill, S., and Fowke, L.C. (2000). Expression of the plant cyclin-dependent kinase inhibitor ICK1 affects cell division, plant growth and morphology. Plant J. **24,** 613–623.

Watt, F.M., and Hogan, B.L. (2000). Out of Eden: Stem cells and their niches. Science **287,** 1427–1430.

Weinl, C., Marquardt, S., Kuijt, S.J.H., Nowack, M.K., Jakoby, M.J., Hulskamp, M., and Schnittger, A. (2005). Novel functions of plant cyclin-dependent kinase inhibitors, ICK1/KRP1, can act non-cell-autonomously and inhibit entry into mitosis. Plant Cell **17,** 1704–1722.

Wohlschlegel, J.A., Dwyer, B.T., Takeda, D.Y., and Dutta, A. (2001). Mutational analysis of the Cy motif from p21 reveals sequence degeneracy and specificity for different cyclin-dependent kinases. Mol. Cell. Biol. **21,** 4868–4874.

Zhang, B., Foley, R.C., and Singh, K.B. (1993). Isolation and characterization of two related Arabidopsis ocs-element bZIP binding proteins. Plant J. **4,** 711–716.

Zhang, F., Gonzalez, A., Zhao, M., Payne, C.T., and Lloyd, A. (2003). A network of redundant bHLH proteins functions in all TTG1-dependent pathways of Arabidopsis. Development **130,** 4859–4869.